Research Article

Marek Kovár*, Marek Živčák, Andrej Filaček, Lucia Jasenovská, Igor Vukelić, Dejana Panković, Viliam Bárek, Xinghong Yang, Marián Brestič

High-throughput digital imaging and detection of morpho-physiological traits in tomato plants under drought

https://doi.org/10.1515/opag-2022-0331
received January 9, 2024; accepted July 2, 2024

Abstract: Advances in informatics, robotics, and imaging techniques make it possible to use state-of-the-art digital reconstruction technologies for high-throughput plant phenotyping (HTPP) affected by stress factors, as well as for the ontology of their structural and functional traits. Digital imaging of structural and functional features of the above-ground part of plants is non-destructive and plants can be monitored throughout their entire life cycle. In the experiment with tomato plants (*Solanum lycopersicum* L.; cv. Gruzanski zlatni) grown in controlled environmental conditions and affected by gradual soil dehydration, we evaluated phenotypic traits and phenotypic plasticity by the PlantScreen^{TM} platform using digital imaging of plant optical signals. In this study, 25 different morpho-physiological traits of the plant were evaluated during the precise control and monitoring of the water content in the soil. Different levels of plant water supply induced statistically significant differences in the formation of individual phenotypic traits. Several plant traits have been identified that are characterized by low variability in both well-hydrated and water-stressed conditions, as well as traits with high phenotypic plasticity. Geometric traits (especially Iso^{top}, Round-2^{top}, and Comp^{side}) showed a relatively low level of drought-induced phenotypic plasticity. However, functional and chemometric characteristics ($\Delta F/F'm$, Rfd, Water-1, and ARI-1) showed the potential to exhibit rapid plasticity in water-stressed conditions. Our results confirmed that a high-throughput phenotyping methodology coupled with advanced statistical analysis tools can be successfully applied to characterize crop stress responses and identify traits associated with crop stress tolerance.

Keywords: high-throughput phenotyping, imaging, chlorophyll fluorescence, chemometrics, tomato, drought

1 Introduction

Environmental stress situations, such as drought, sub- and supra-optimal temperature, salinity, etc., significantly affect plant productivity. Drought in the context of ongoing climate change is one of the most frequently occurring constraints, resulting in a reduction of plant growth, development, and yield [1]. The urgency of studying the agrobiological consequences of drought on the molecular, physiological, and yield-forming processes of crops is also compounded by the increasing need for food [2]. Nowadays, many sophisticated tools are available to researchers studying plant responses to various stress situations, including drought [3]. Advances across multiple omics techniques open new possibilities for a comprehensive description of the mechanisms of plant reactions to stress [4–6].

Under drought stress, many physiological processes are affected, such as leaf expansion [7], stomatal behaviors [8], photosynthesis, transpiration, source-sink relationship, and translocation of assimilates [9–12], resulting in both root and shoot growth. The complexity of plant responses to drought has been observed. Drought tolerance in plants is manifested by effects such as scavenging of reactive

*** Corresponding author: Marek Kovár,** Institute of Plant and Environmental Sciences, Slovak University of Agriculture, A. Hlinku 2, 94976, Nitra, Slovak Republic, e-mail: marek.kovar@uniag.sk, tel: +421-37-641-4440
Marek Živčák, Andrej Filaček, Lucia Jasenovská, Marián Brestič: Institute of Plant and Environmental Sciences, Slovak University of Agriculture, A. Hlinku 2, 94976, Nitra, Slovak Republic
Igor Vukelić: Faculty of Ecological Agriculture, Educons University, Vojvode Putnika 87, 21208, Sremska Kamenica, Serbia
Dejana Panković: Julius Kuehn Institute, Institute for Resistance Research and Stress Tolerance, Erwin Baur Strasse 27, 06484, Quedlinburg, Germany
Viliam Bárek: Institute of Landscape Engineering, Slovak University of Agriculture, A. Hlinku 2, 94976, Nitra, Slovak Republic
Xinghong Yang: National Key Laboratory of Wheat Improvement, College of Life Science, Shandong Agricultural University, Taian, 271018, China

oxygen species, osmotic adjustment, changes in membrane lipid composition and hormonal balance, and modulation of photosynthesis and water use efficiency [11,13–16]. These characteristics of plant drought tolerance are widely used in plant stress physiology, crop breeding, and agronomy. However, the quantification of these signs is time-consuming, often destructive, difficult to carry out simultaneously, and requires experienced personnel capacities (e.g., [17,18]). These are the main reasons why we are looking for new, quick, and expeditious techniques that will enable a reliable quantitative description of plant phenotypic traits and screening criteria, reflecting the mechanisms of plant tolerance to abiotic stress situations.

In contrast to the current genomic analyses using next-generation sequencing, the bottleneck in the selection of biological material and stress-induced phenotype plasticity is the quantitative description of the plant phenome [19,20]. Recent progress in the construction and application of optical-based plant phenotyping techniques allows non-destructively and quickly a large number of individuals, as well as many structural and functional plant traits [17,21,22]. A key benefit of high-throughput plant phenotyping (HTPP) is the non-destructive imaging and computer vision of plant optical signals, which allows the creation of time series measurements of individual plant traits at high resolution and high precision. Over the last two decades, dozens of automated phenotyping installations have been created worldwide, which are capable of characterizing plant performance and phenotypic plasticity in various fully regulated or semi-regulated environmental conditions [23–31]. HTPPs enable the screening of biological material of many plant species tolerant to stress situations by focusing on the quantification of architecture [27] and biomass-related traits [30], photosynthetic performance [32], water, light, and nutrient use efficiency, respectively [26,31], content of biologically active substances [20,33,34] and water [35], etc. High correlations between the digital RGB determined of shoot or leaf area and the shoot fresh/dry biomass weights, respectively, were reported in many plants, including *Arabidopsis*, tobacco, wheat, rice, and tomato [23,26,32]. RGB-based phenotyping also allows many morphometric features of the plant to be evaluated, such as height, compactness, or isotropy [36]. To reveal spatial heterogeneity of the photosynthetic activity, chlorophyll fluorescence imaging can be used [37]. Hyperspectral spectroscopy of plant reflectance has become a highly valued technique for evaluating biologically active substances and water in tissues [33–35,38].

The high-throughput phenotyping PlantScreen^{TM} platform, installed in the Laboratory of Production Physiology and Plant Ecophysiology of the AgroBioTech Research Centre at the Slovak University of Agriculture in Nitra, enables the use RGB, chlorophyll a fluorescence, and hyperspectral reflectance spectroscopy sensors, in the quantitative description of the structural and functional features of the phenotype of plants grown in controlled environmental conditions. The aim of this pilot study originating from this platform was to demonstrate the utility of phenotyping installation in describing drought-induced phenotypic changes in tomato plants, as well as quantify the variability of the obtained data during the entire experiment, and identify the magnitude of phenotypic plasticity by comparing changes in the values of a total of 25 structural, functional, and chemometric traits.

2 Material and methods

2.1 Plant material and cultivation

Tomato seeds (*Solanum lycopersicum* L.; cv. Gruzanski zlatni) were sowed into plastic cultivation plate pots (6 × 4 pots; filled with peat substrate TS2 (Klasmann-Deilmann, Geeste, Germany). Germination of plants took place at 250 μmol m^{-2} s^{-1} light intensity and 14 h/10 h (day/night) photoperiod, temperature 25°C/17°C (day/night), and air humidity 60%. After plant emergence, plants were transplanted to 5-L plastic pots filled with TS2 substrate, and 40 pots were registered into the PlantScreen^{TM} conveyor phenotyping platform (PSI, Drásov, Czech Republic). The phenotyping platform consists of cultivation space and units containing optical sensors (two RGB, one chlorophyll a fluorescence, and two hyperspectral spectrometers); sensor configuration, and the cultivation area with tomato plants, as shown in Figure 1. Experimental trays (well-watered – WW and water-stressed – WS, respectively) were kept in the cultivation area of the platform for the completely randomized design. For phenotyping, we used nine plants in the WW experimental group and 15 plants in the WS group. Plants were 48 days cultivated under fully regulated environmental conditions, such as light intensity 1,000 μmol m^{-2} s^{-1} (cool white light, dark red light, and far-red light at the proportion of 80, 10, and 10% total light intensity, respectively, measured with spectrophotometer SpectraPen mini, PSI, Drásov, Czech Republic), 14 h/10 h (day/night) photoperiod, air temperature of 25°C/17°C (day/night), air humidity of 40–53%, and ambient CO_2 concentration (350–400 ppm). The recorded parameters of the environmental conditions during plant cultivation are shown in Figure 2. Water irrigation was controlled gravimetrically (±2.0 g) using weighing and irrigation station of phenotyping PlantScreen^{TM} platform

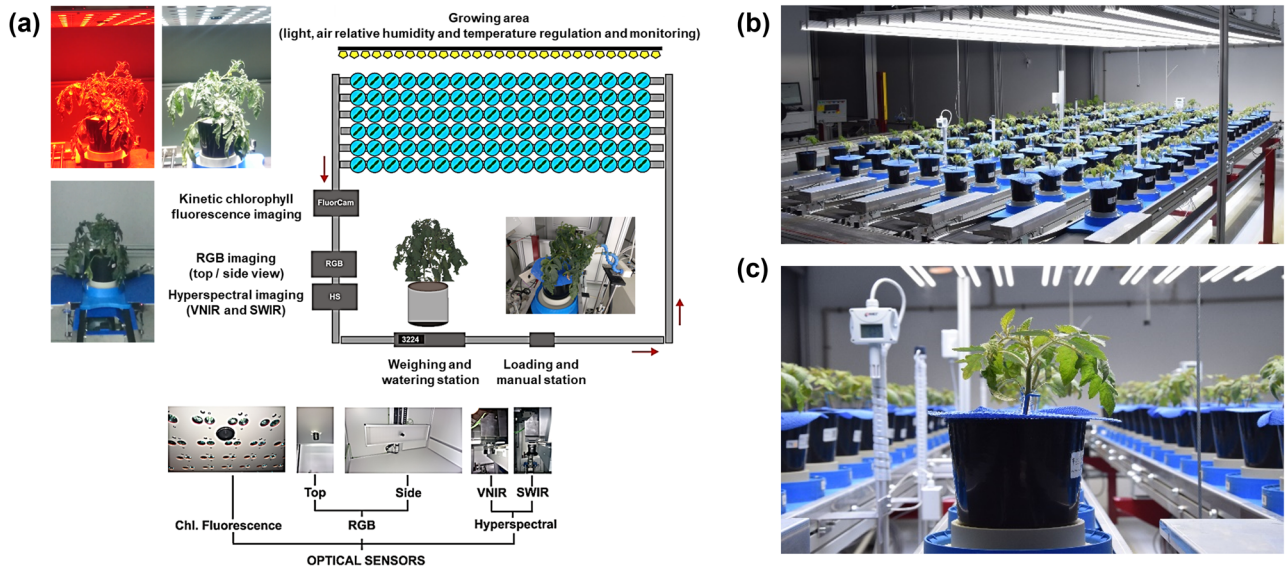

Figure 1: (a) Sensors configuration in high-throughput phenotyping platform PlantScreen^{TM}, (b) tomato plants on conveyor belts in the cultivation area phenotyping platform, and (c) detail photography of tomato plant.

into 70% of full soil water capacity (SWC; reference weight 1,490 g). Plants watered in this protocol were referred to as WW. After the acclimatization period (9 DAE) to environmental conditions and the plant phase period of the third fully developed leaves, the dehydration cycle of randomly selected pots with tomato plants (WS) was initiated by water withholding up to the level of 15% SWC. SWC was calculated by the equation [39]:

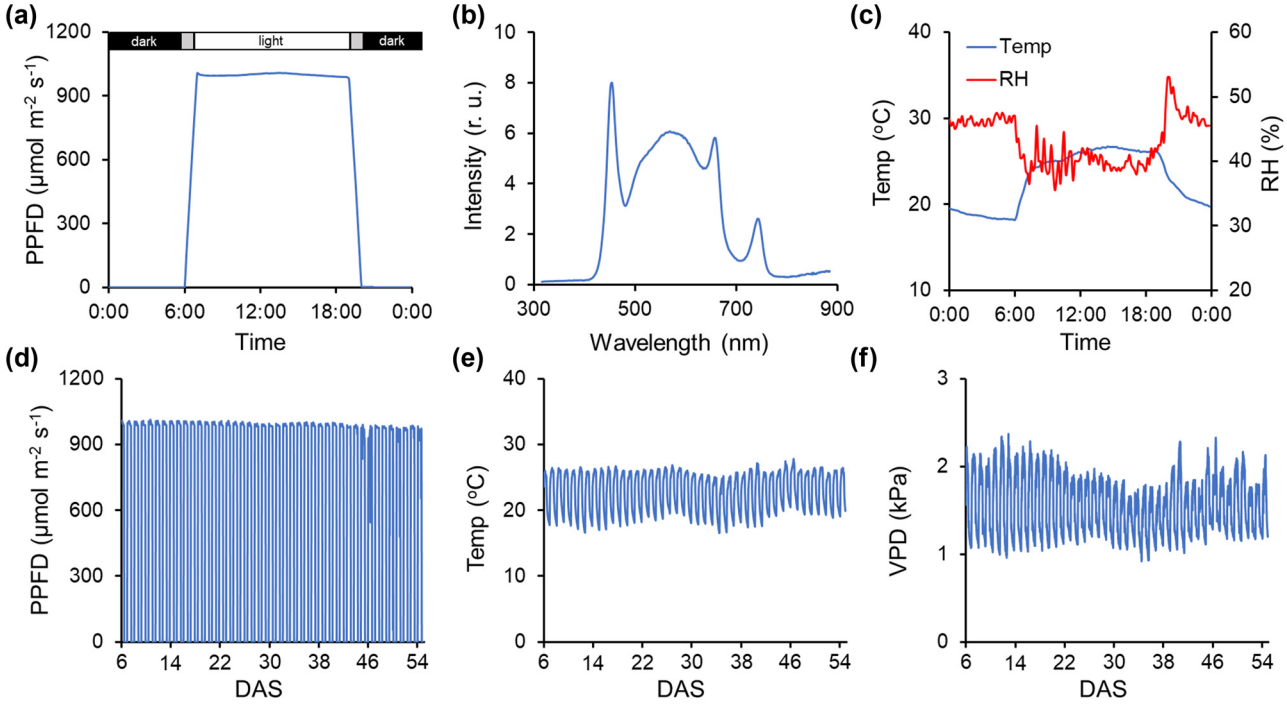

Figure 2: Microclimatic parameter during cultivation of tomato plants: (a) one-day record of intensity of irradiance (PPFD), (b) spectral characteristics of irradiance, (c) air temperature (Temp) and relative humidity (RH) during the day, (d) course intensity of irradiance (PPFD), (e) air temperature (Temp), and (f) air vapor pressure deficit (VPD) during the experiment. DAS – day after sowing.

$$SWC = \frac{WW - DW}{DW}$$

where WW is the wet weight of the substrate, and DW is the dry weight of the substrate after drying in an oven at 105°C until constant weight. Soil WW was determined 10 h after full watering of substrate in pots (100% field water capacity) [39].

2.2 Data acquisition

Images collection was programmed using PlantScreen™ Scheduler software (PSI, Drásov, Czech Republic). For RGB imaging, plants were imaged each second day using both RGB sensors in top and side configuration. The technical specifications of the sensors used are described in Table 1. Briefly, color images (5 MPx) were recorded from the top view (top of the plant) and scanned from the side at two angles (0 and 90 degrees, respectively). Recorded images (resolution 2,560 × 1,920 Px) were stored in the database and processed using PlantScreen™ Data Analyzer (PSI, Drásov, Czech Republic).

The method of quantifying chlorophyll a fluorescence has become an important tool that allows the evaluation of the performance of primary photosynthetic reactions in different growing environmental conditions. Thus, the photosynthetic performance of plants was analyzed (every fourth day on average) by chlorophyll a fluorescence (CF) imaging using FluorCam FC-800MF fluorometer (technical specifications are shown in Table 1) working at pulse amplitude mode (PSI, Drásov, Czech Republic). Plants were loaded into the CF unit during the night (starting at 10:00 pm) in a dark-adapted state of photosystem II. For the calculation of photosynthetic performance, the protocol of quenching analysis with the intensity of 600 μmol m^{-2} s^{-1} cool white actinic light was used.

VNIR (visible and near-infrared region) and SWIR (short-wavelength infrared region) spectrometer (HC) at top view configuration were used for hyperspectral reflectance analysis. Technical specifications for both sensors are shown in Table 1. First, dark and light (Spectralon plate) calibration images were performed before HC imaging. Both HC imaging spectrometers (VNIR and SWIR) produce a 2D spatial array of vectors that represent the spectrum at each pixel location of the image. The resulting 3D datacubes of the image contain two spatial dimensions (axes *x* and *y*) and one spectral dimension (*z*-axis). Plants were loaded into the HC unit and illuminated by one halogen tube (600 W, color temperature of 2,600 K). VNIR and SWIR sensors perform images in line with scanner operation.

2.3 Data pre-processing and image extraction

For RGB, PlantScreen™ Data Analyzer software (PSI, Drásov, Czech Republic) performed three steps to plant image extraction and subsequent calculation of plant growth and morphological parameters. In the first step of RGB image pre-processing, the correction of barrel distortion was automatically performed, followed by background subtraction to remove non-plant pixels, plant mask preparation by image binarization, and finally, RGB reconstruction of the image in native and artificial colors. The second step of data processing included the calculation of plant area and morphological parameters. Raw CF image pre-processing was automatically performed consisting of plant mask application, background subtraction, and finally pixel-by-pixel CF parameter calculation was done. Acquired hyperspectral data from both VNIR and SWIR sensors were processed using pixel-by-pixel analysis, featuring radiometric and dark noise calibration, background subtraction, and automated vegetation indices computation. Plant mask during HC image pre-processing for each image was constructed from VNIR datacube using math formula:

Table 1: Technical specifications of sensors for RGB, chlorophyll a fluorescence (CF), and hyperspectral reflectance (HC) imaging

	RGB sensor	CF sensor	HC sensor VNIR	HC sensor SWIR
Sensor technology	CMOS color 1/2″	1/2″, mono	Silicon	InGaAs
Resolution	5.00 MPx			
Effective pixels	2,560 × 1,920	720 × 560	640 × 480	640 × 480
Pixel size	2.2 μm	8.6 × 8.3 μm	25 μm	25 μm
Interface	GigE	GigE	GigE	GigE
Spectral range			340–900 nm	900–1,700 nm
Image frequency		50 fps	50 fps	50 fps

$$\text{Plant pixel} = 1.2 \times [2.5 \times (R^{740} - R^{672}) - 1.3 \times (R^{740} - R^{556})]$$

where R^{740}, R^{672}, and R^{556} are values of reflectance intensities at 740, 672, and 556 nm.

Calculations and brief descriptions of individual calculated parameters (geometrical, structural, and chemometric) are shown in Table 2.

Evapotranspiration rate (ET; g $H_2O\,dm^{-2}\,day^{-1}$) was calculated for each plant and each day according to equation [40]:

$$ET_i = \frac{(WA - WB)}{A} \times \frac{1}{t_k}$$

where WA is the pot weight before watering at day t_i, WB is the pot weight after day t_{i-1}, A is the aboveground plant area at t_i and t_i is the day of interest and t_{i-1} is the previous day.

2.4 Statistical analysis

Plant structural and functional traits data extracted from images were analyzed using Statistica software version 10 (StatSoft Inc., Tulsa, OK, USA), the statgenHTP Package and

Table 2: Parameter description of structural, functional, and chemometrics plant traits used in this study

Parameter	Description	Calculation
Structural parameters		
A	Aboveground plant area, calculated as the integral volume of plant pixels in three image projections (top view and side view at 0, and 90 degrees	$A = \sqrt{(A^{top})^2 + (A^{side\_0})^2 + (A^{side\_90})^2}$
P^{top}	Length of the plant perimeter top view	—
P^{side}	Length of the plant perimeter side view	—
$Comp^{top}$	Compactness top view	$Comp^{top} = A^{top}/\text{convex hull } A^{top}$
$Comp^{side}$	Compactness side view	$Comp^{side} = A^{side}/\text{convex hull } A^{side}$
$Round^{top}$	Roundness	$Round^{top} = 4{\cdot}\pi{\cdot}A^2/P^2$
Round-2^{top}	Roundness-2	$Round\ \ 2^{top} = 4{\cdot}\pi{\cdot}A^2/P\text{convex hull}^2$
Iso^{top}	Isotropy	$Iso^{top} = 4{\cdot}\pi{\cdot}A^2/P\text{polygon}^2$
Ecc^{top}	Eccentricity	$Ecc^{top} = 2{\cdot}\left\{\sqrt{\left[\left(L^{major}/2\right)^2 - \left(L^{minor}/2\right)^2\right]}\right\}L^{major}$
RMS	Rotational mass symmetry	$RMS = (Area^{circle} + Area^{convex\ hull})/(Area^{circle} - Area^{convex\ hull})$
SOL	Slenderness of leaves	$SOL = P\text{skeleton}^2/A^{top}$
H	Height of bounding box enveloping plant	—
W	Width of bounding box enveloping plant	—
Functional photosynthetic parameters		
Fo	Minimal intensity of chlorophyll a fluorescence at dark	—
Fm	Maximal intensity of chlorophyll a fluorescence at dark	—
Fp	Peak fluorescence during initial phase of Kautsky effect	—
Fs	Instantaneous fluorescence (steady-state) at light	—
F´m	Maximal intensity of chlorophyll a fluorescence at light	—
Fv/Fm	Maximal photochemical efficiency of PSII at dark	$Fv/Fm = \frac{(Fm - Fo)}{Fm}$
$\Delta F/F'm$	Actual photochemical efficiency of PSII at light	$\Delta F/F'm = \frac{(F'm - Fs)}{F'm}$
NPQ	Non-photochemical quenching of fluorescence	$NPQ = (Fm - F'm)/F'm$
Rfd	Relative fluorescence decline	$Rfd = (Fp - Fs)/Fs$
Chemometrics VNIR and SWIR parameters		
NDVI	Normalized difference vegetation index	$NDVI = R^{800} - R^{670}/R^{800} + R^{670}$
MCARI-1	Modified chlorophyll absorption ratio index 1	$MCARI\ \ 1 = 1.2{\cdot}[2.5{\cdot}(R^{800} - R^{670})\ \ 1.3{\cdot}(R^{800} - R^{550})]$
CHLa	Chlorophyll a reflectance index	$CHLa = R^{776}{\cdot}[(1/R^{673}) - 1]$
ARI-1	Anthocyanin reflectance index 1	$ARI\ \ 1 = 1/R^{550} - \frac{1}{R^{700}}$
CRI-1	Carotenoid reflectance index 1	$CRI\ \ 1 = 1/R^{510} - \frac{1}{R^{550}}$
Water-1	Water reflectance index 1	$Water\ \ 1 = R^{1,440}/R^{960}$

Outlier Detection Methods (both from EPPN2020 project) tools of R-Studio (Posit, PBC, Boston, USA). In the first step, the results were analyzed with the Grubbs test, which identifies outliers between individual biological replicates in each genotype and treatment according to Poudel et al. [41]. The threshold for outliers and extreme values was done as 2·S.D using statgenHTP Package and Outlier Detection Methods. Subsequently, Laven's and Cochran's statistical tests were used to evaluate data homogeneity and distribution of normality using Statistica software. Statistically significant differences were subjected to analysis of variance (ANOVA) at the significance level of 0.05 and then to Tukey *post-hoc* test and indicated as $p < 0.05$*, 0.01**, and 0.001***.

Correlation relationships between individual traits were assessed by Pearson's correlation coefficient (r_P). The evaluation of the degree of trait variability was calculated as the coefficient of variability (C.V.; dimensionless unit) according to the equation:

$$\text{C.V.} = \frac{\sigma}{\mu}$$

where σ is the standard deviation and μ is the mean.

The magnitude of the phenotypic plasticity of an individual trait (PhP) was calculated according to the equation [42]:

$$\text{PhP}_i = \frac{x_i^{\text{WS}} - x_i^{\text{WW}}}{x_i^{\text{WW}}} \times 100$$

where x_i^{WW} is the mean value of the individual trait in WW plants and x_i^{WS} is the mean value of the individual trait in WS plants.

3 Results and discussion

The realization of genetic information in the ontogenetic program of the plant and the phenotype expression are performed in direct connection and interaction with the environment. A long-term goal of plant biologists and physiologists is to study and interpret the structural and functional dynamics of plant organisms using a non-invasive imaging approach. Digital phenotyping is becoming a popular tool for the quantitative description of structural and functional traits of plants, especially those related to biomass production and stress tolerance. An essential part of the quantitative description of the phenotype is the knowledge of the microclimatic conditions of the environment in which plant growth and development take place.

At the stage of the third fully developed tomato leaf (9 DAE), the dehydration cycle was started by water withholding of soil substrate (Figure 3a). In well-watered (WW) plants, the SWC (soil water content) level was maintained at 70%. In water-stressed (WS) plants, SWC was continuously decreasing, and a level of 15% SWC was reached after 17 days of gradual substrate dehydration, corresponding to a mean rate of 3.2% water loss. It is well documented in the literature that slow and gradual dehydration of the substrate allows plants to develop protective responses against drought and increase the degree of drought resistance [11,42].

Drought resistance has been identified as a "complex trait" [43], and the most important resistance traits ensure hydration and tissue turgor maintenance. In plants, turgor pressure plays an essential role in critical processes such as growth, development, mechanical support, signaling, organ movement, flowering, and plant stress responses [44]. During evolution, plants under selection pressure have developed evolutionary strategies to cope with drought through phenotypic plasticity [45]. The observed stress-induced higher value of phenotypic plasticity (PhP) leads to more significant differences in the expression of phenotype between WW and WS plants. A total of 25 plant traits were quantified in this study and divided into three classes: structural, functional, and chemometrics (Table 3). It was identified that the area growth rate of well-hydrated plants shows a typical sigmoidal course (Figure 3b), and the aboveground plant area reached a level of 22.96 dm^2. As expected, drought causes a statistically significant reduction in growth, with a visually observable phenotypic expression as early as 25 DAE (Figure 3c). The drought significantly and negatively impacted the formation of the vertical architecture of the plant (Table 3). Plant height (H), compactness ($Comp^{top}$), and slenderness of leaves (SOL) are considered the most important geometrical parameters of the vertical structure of plants, which sensitively reflect plant growth disturbances and leaf area evolution under stressful situations. The phenotypic expression of these traits is relatively uniform between plant individuals growing in a given environment (WW and WS), which is documented by the low value of variability (C.V. from 0.04 to 0.15 dimensionless unit) and the high value of partial η^2 (Table 3). In this experiment, it was observed that the phenotypic manifestation of traits describing the geometry and vertical structure of adult tomato plants is more complex than that of plant species in juvenile stages of ontogenesis [46] and/or forming a small number of leaves [47] or finally such plants that form a rosette of leaves [36].

Using the precision weighing and irrigation station of the PlantScreen™ phenotyping system, the rate of

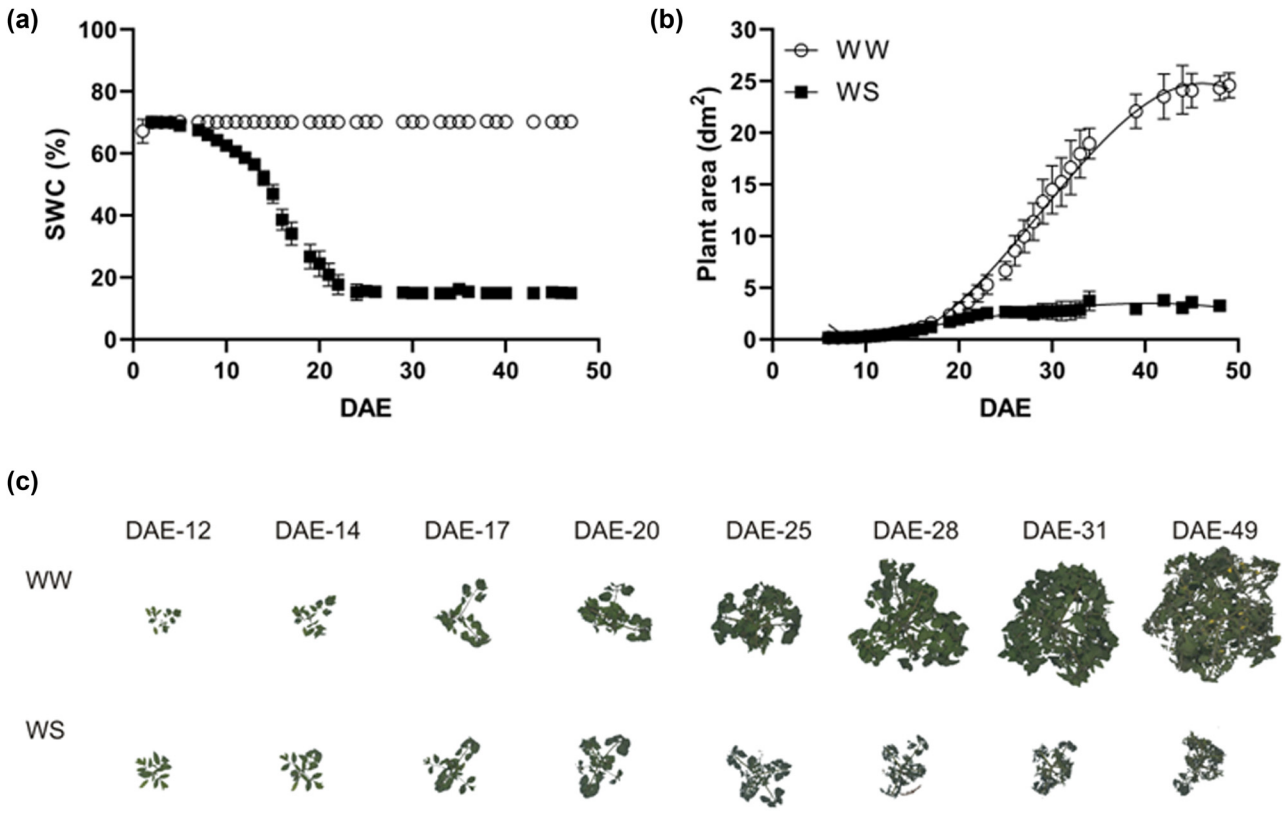

Figure 3: Dynamics of soil water content (SWC) (a) and growth of shoot area in well-watered (WW) and water-stressed (WS) tomato plants (b). DAE – day after emergency. Point represented mean ± SD (n = 9–15). (c) Ontology of RGB imaging of WW and WS plants.

Table 3: Effect of well-watered (WW) and water-stressed (WS) conditions on structural, functional, and chemometrics traits

Parameter	WW	WS	*P*	partial η^2	PhP
A (dm^2)	22.96 ± 2.30	3.26 ± 0.21	***	0.998	−85.80
P^{top} (dm)	10.53 ± 3.72	3.98 ± 1.32	***	0.925	−62.20
P^{side} (dm)	74.13 ± 8.52	46.09 ± 6.28	***	0.802	−37.83
Comp^{top}	0.606 ± 0.027	0.369 ± 0.030	***	0.951	−39.11
Comp^{side}	0.653 ± 0.194	0.483 ± 0.040	*	0.306	−26.03
Round^{top}	0.046 ± 0.007	0.031 ± 0.005	***	0.638	−32.61
Round-2^{top}	0.899 ± 0.042	0.813 ± 0.050	**	0.490	−9.57
Iso^{top}	0.258 ± 0.027	0.226 ± 0.022	*	0.243	−12.40
Ecc^{top}	0.163 ± 0.037	0.536 ± 0.101	***	0.865	228.83
RMS	0.390 ± 0.063	0.677 ± 0.085	***	0.802	73.59
SOL	2262.86 ± 299.74	615.70 ± 77.86	***	0.944	−72.79
H (dm)	5.28 ± 2.47	2.80 ± 0.36	**	0.371	−46.97
W (dm)	4.86 ± 0.71	1.98 ± 0.10	***	0.907	−59.26
Fo	119.49 ± 10.65	85.34 ± 5.85	***	0.816	−28.58
Fm	651.77 ± 39.59	350.12 ± 48.01	***	0.930	−46.28
Fv/Fm	0.833 ± 0.014	0.780 ± 0.018	***	0.754	−6.36
$\Delta F/F'm$	0.226 ± 0.015	0.130 ± 0.022	***	0.879	−42.48
NPQ	0.924 ± 0.101	0.590 ± 0.129	***	0.701	−36.15
Rfd	1.388 ± 0.195	0.798 ± 0.190	***	0.730	−42.51
Water-1	0.326 ± 0.038	0.870 ± 0.078	***	0.957	166.87
NDVI	0.785 ± 0.030	0.690 ± 0.036	***	0.695	−12.10
MCARI-1	0.622 ± 0.046	0.391 ± 0.078	***	0.784	−37.14
CHLa	9.245 ± 0.871	14.078 ± 1.289	***	0.845	52.28
ARI-1	0.718 ± 0.267	2.860 ± 0.488	***	0.893	298.33
CRI-1	8.715 ± 1.032	15.732 ± 1.216	***	0.916	80.52

P – probability by Tukey's *post-hoc* test at 0.05*, 0.01**, and 0.001***; PhP – phenotypic plasticity.

evapotranspiration (ET) was calculated during the ontogeny of tomato plants (Figure 4). ET was investigated in more detail in an experiment at regular two-day intervals to understand the causal significance of the physiological and morphological responses of drought-stressed tomato plants. At the beginning of ontogenesis, we determined the rate of water evaporation from the plant and the soil surface at the level of 147 ± 11 g H_2O per dm^2 leaf area and day. During the growth of the plant's leaf area, we observed a significant decrease in ET (nearly 35% reduction) even in WW, which can be attributed to the progressive formation of the plant cuticle [48], and optimization of stomatal behavior [49], or the reduction of water evaporation from the soil surface due to the increase in plant size (Figure 3b and c). At the time when the level of SWC in WS plants reached the value of 15%, ET was at the level of 20 ± 5 g dm^{-2} day^{-1}. A similar ontogenetic variation of ET was observed in wheat plants by a previous study [32], but unlike that, our simultaneous phenotyping of plants together with digital assessment of leaf area allows the calculation of water loss per unit leaf area. Despite the fact that image-based RGB phenotyping is intensively used in the description of the structural features of the phenotypes of many plant species, as far as we know, there are only a few comprehensive studies that would comprehensively describe the anatomical traits of the visual manifestation of plant morphology. In addition to the water content in the soil, the vapor pressure deficits (VPD) play an important role in shaping the anatomy of the tissues and the morphology of the plant. As an example, Amitrano et al. [50] use the combination of image-based phenotyping with in-depth anatomical analysis in the study of lettuce plant responses to drought and VPD.

The technique was and still is successfully used in basic photosynthetic research, but it has also found applications in screening in breeding [10,51]. The formation of functional traits of plant photosynthetic performance during ontogenesis in WW and WS is shown in Figure 5. The minimal (Fo) and maximal (Fm) chlorophyll a fluorescence intensity during plant ontogeny increases slightly in WW. A generally observed response to drought is a decrease in both Fo and Fm, respectively. In our experiment, it was observed that WS induced a statistically significant ($p < 0.001$) decrease in Fo and Fm from day 16 of water stress, and Fo responds faster and more sensitively to stress (Figure 5a and b). This acclimation response is attributed to the induction of photoprotective mechanisms and/or damage to PSII photosystems [52].

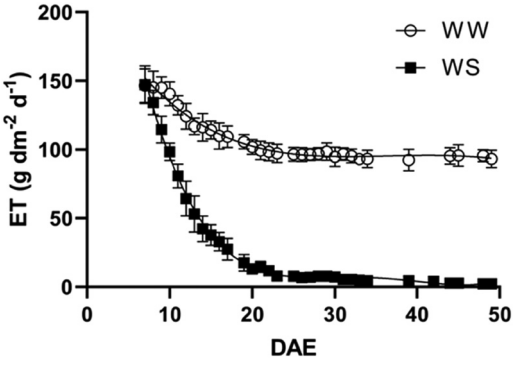

Figure 4: Evapotranspiration rate (ET; g dm^{-2} day^{-1}) in well-watered (WW) and water-stressed (WS) tomato plants. DAE – day after emergency. Point represented mean ± SD (n = 9–15).

The maximal PSII photochemical efficiency (Fv/Fm) is a good indicator of plant responses to many stress situations [51]. However, Fv/Fm is relatively stable in many plant species, including tomatoes, under moderate drought conditions, with a decrease only under severe drought [53,54]. The maximal photochemical efficiency of PSII (Fv/Fm) was observed to increase slightly above the value of 0.830 in the first phase of plant ontogenesis (Figure 5c). In WS plants, a decrease in the value of Fv/Fm was observed only from the twenty-first day of dehydration, when the plants had already been grown for 10 days at 15% SWC. At the end of the dehydration cycle, Fv/Fm dropped significantly ($p < 0.001$) to 0.780 ± 0.018 (Table 3).

Since the method of whole-surface imaging of chlorophyll a fluorescence documents the mean level of Fv/Fm from the whole plant [24], we confirmed the heterogeneities between the individual leaves. Figure 5g also documents this fact. A much more sensitive parameter that describes the primary reactions of photosynthesis under stress is the actual PSII photochemical efficiency (ΔF/F′m). In WW, ΔF/F′m increased during plant ontogeny (Figure 5d). A drought-induced decrease in ΔF/F′m was observed in WS plants already on the 5th day of dehydration ($p < 0.001$). Parameter ΔF/F′m reflects both the maximum photochemical efficiency of PSII at actinic light and the efficiency of thermal dissipation of excitation energy by non-photochemical processes (NPQ). The highest level of non-photochemical quenching of chlorophyll fluorescence (NPQ) was observed in juvenile tomato plants (1.40 ± 0.10). During ontogenesis, NPQ decreased more in plants affected by water stress [0.924 ± 0.101 in WW vs 0.590 ± 0.129 in WS; $p < 0.001$ (Table 3)]. A significant dehydration-induced decrease in NPQ level ($p < 0.001$) of the whole plant compared to WW appeared on the eleventh day of drought (Figure 5e). A surprising finding is that the formation of the plant's assimilation surface was accompanied by a decrease in the NPQ value during ontogenesis. It nicely illustrates that imaging of NPQ during ontogenesis allows the efficient visualization of physiological processes and activities, including related

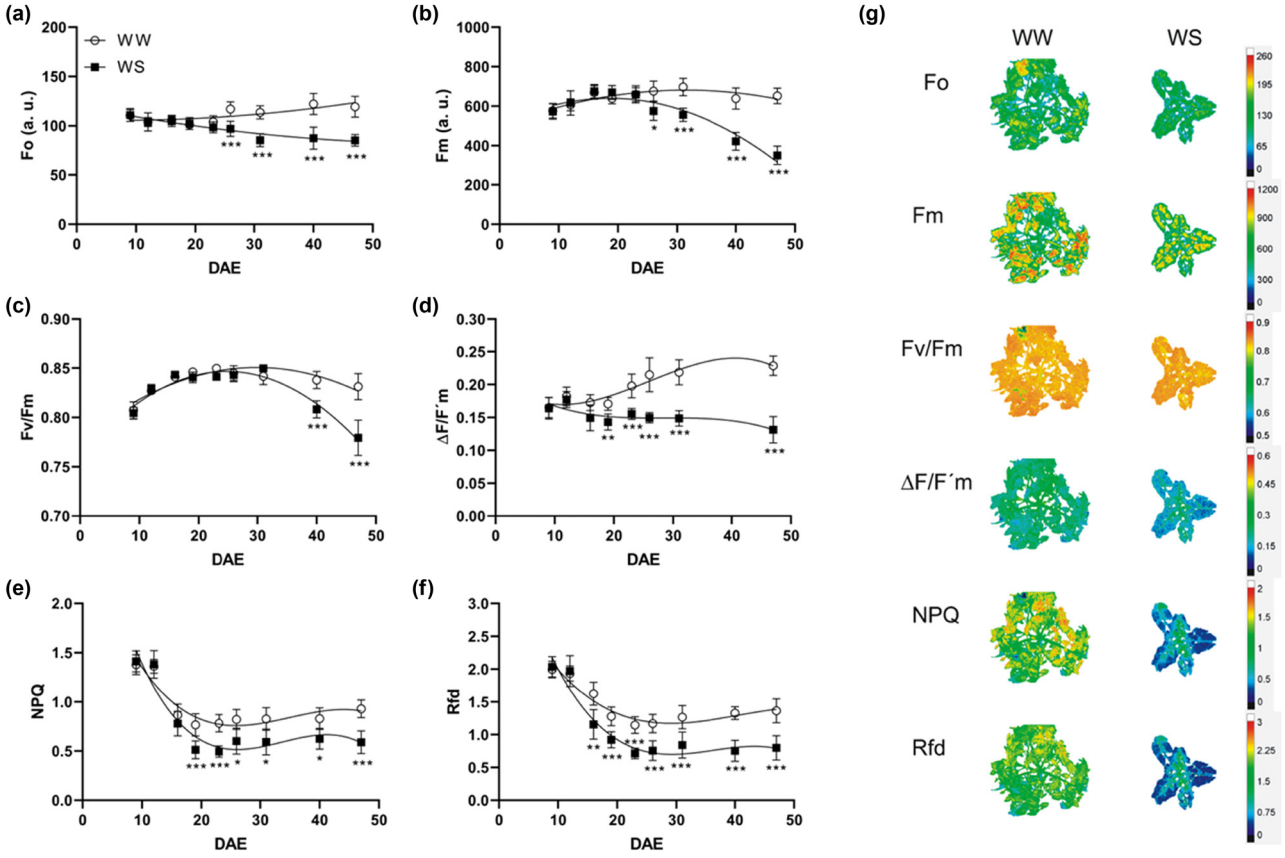

Figure 5: Dynamic light energy conversion into photochemical and non-photochemical processes in tomato plants growing in well-watered (WW) and water-stressed (WS) conditions. (a) minimal intensity of fluorescence (Fo), (b) maximal intensity of fluorescence (Fm), (c) maximal efficiency of PSII photochemistry at dark (Fv/Fm), (d) actual efficiency of PSII photochemistry at light (Δ*F*/F′m), (e) non-photochemical quenching of fluorescence (NPQ), (f) relative fluorescence decrease (Rfd) and (g) heterogeneity of photosynthesis functionality expressed by full-screen imaging of chlorophyll a fluorescence parameter. Parameters were calculated as the mean value of all pixels from plant chlorophyll fluorescence imaging. DAE – day after emergency. Point represented mean ± SD (n = 9–15). Statistical differences are determined by Tukey *post-hoc* test and indicated as p < 0.05*, 0.01**, 0.001***.

heterogeneities. Higher activity of thermal dissipation of excitation energy was observed in ontogenetically younger (upper) leaves than in ontogenetically older (lower) leaves. Thus, our results efficiently contribute to the knowledge of plant species-dependent ontogenetic changes in NPQ that are well documented in the literature [55,56].

Parameter Rfd (relative fluorescence decline) is directly correlated with the net CO_2 assimilation rate of leaves of many plants affected by different environmental conditions [57]. Like the NPQ parameter, the highest level of the Rfd was observed in juvenile tomato plants (2.016 ± 0.138). During ontogeny, the total Rfd level of the whole plant decreased rapidly (up to 22 DAE) and maintained a stable level in both WW and WS plants. Finally, water stress resulted in a significant decrease (p < 0.001) in Rfd, with higher activity in younger than older leaves (Figure 5f and g).

Hyperspectral reflectance is an excellent tool for quantifying changes in the content of biologically significant substances in plant leaves during stress situations [12,33,35]. Non-destructive chemometrics using VNIR and SWIR hyperspectral sensors installed in PlantScreen^{TM} platform allowed us to evaluate the drought-induced kinetics of changes in water content (Water-1), assimilation pigments (NDVI, MCARI-1), chlorophyll a (CHLa), carotenoids (CRI-1), and anthocyanins (ARI-1) in tomato leaves (Table 3 and Figure 6). As drought increases, the water-1 parameter increases and is strongly (negatively; r_P = −0.84; p < 0.001) correlated with SWC (Figures 6a and 7b), and low variability (C.V.) was observed within both the treatment (Figure 7a). These results show that using the SWIR sensor for water content assessment is more accurate than using VNIR indices [35]. The indices quantifying the content of assimilation pigments (NDVI and MCARI-1) showed the lowest phenotypic

plasticity from the chemometric parameters. On the other hand, drought stress induced an almost threefold increase in the concentration of anthocyanins (ARI-1) in tomato plants.

A significant benefit of using modern automatic phenotyping platforms evaluating many morphological and physiological parameters is the quantification of the phenotypic plasticity (PhP) of the trait (Table 3). The PhP is characterized by the ability of an organism to undergo reversible morphological, biochemical, or physiological changes in response to environmental conditions [45]. In this study, some geometric traits show relatively low levels of drought-induced PhP (especially Iso^{top}, Round-2^{top}, and $Comp^{side}$) ranging from −9.57 to −26.03; these are still higher values than those reported in earlier literature [46]. A negative value of the calculated PhP means a reduced level of the given trait due to drought. It was observed in our experiment that in contrast to geometrical traits, functional and chemometrics traits have the potential to exhibit rapid plasticity in WS conditions. This mainly concerns drought-induced changes in the contents of chlorophyll a (CHLa), carotenoids (CRI-1), and anthocyanins (ARI-1, identified PhP values from 50 to 300), which is given by both strength and duration of stress. Evaluation of the phenotypic plasticity of morphological and physiological traits has applications in breeding strategies for creating new biological material for tomatoes tolerant to drought [11,49,58]. Thus, in breeding programs, the selection of genotypes based on traits with lower phenotypic plasticity could help to increase production performance under drought conditions.

Finally, the sensitivity of assessing plant responses to drought through digital phenotyping was supported by correlation analysis (Figure 7b), which confirmed a very

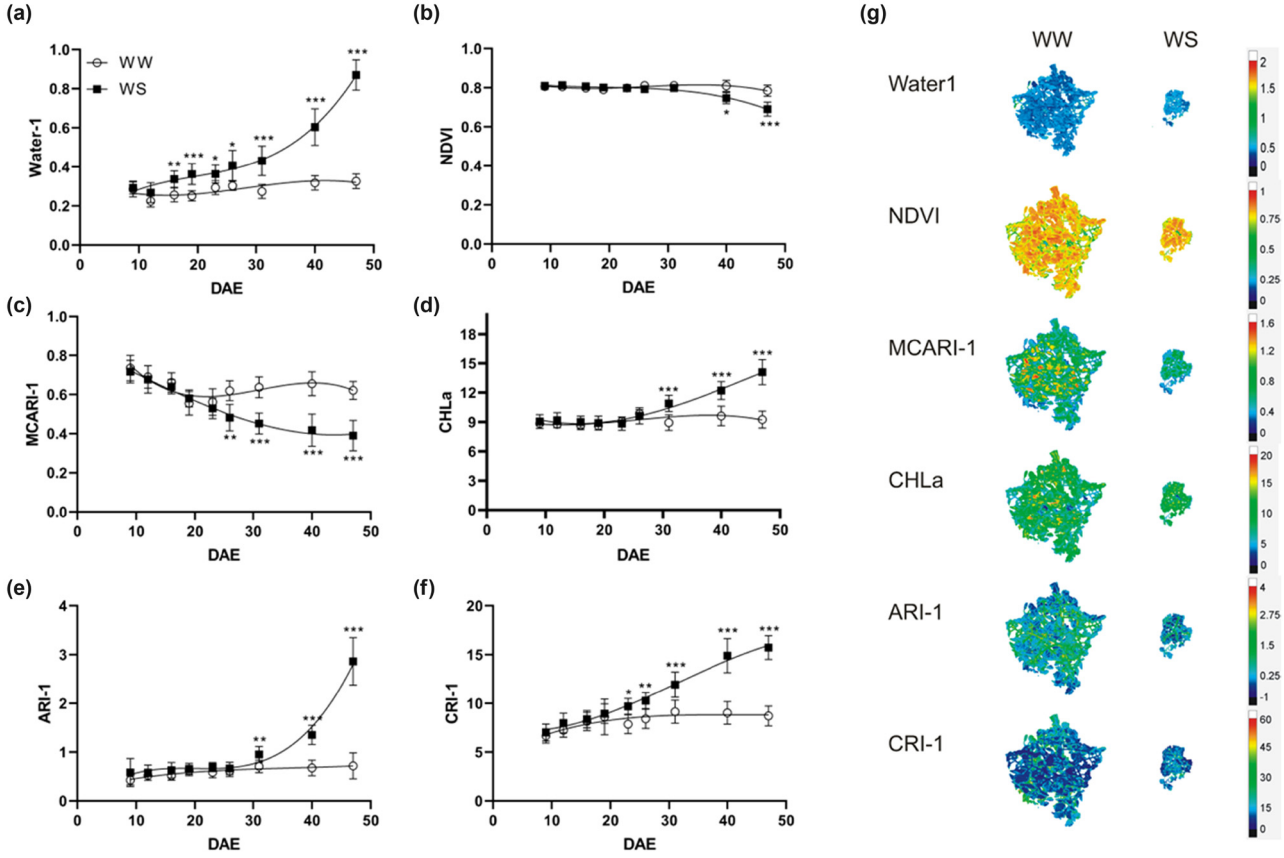

Figure 6: Heterogeneity of functional parameters of chemometrics expressed by full-screen imaging of hyperspectral SWIR and VNIR reflectance parameters well-watered (WW) and water-stressed (WS) tomato plants at terminal stages of dehydration cycle (DAS = 47). (a) Water-1 index, (b) normalized difference vegetation index (NDVI), (c) modified chlorophyll absorbance ratio index (MCARI-1), (d) chlorophyll an index (CHLa), (e) anthocyanin reflectance index (ARI-1), (f) carotenoid reflectance index (CRI), and (g) heterogeneity of chemometrics values expressed by full-screen imaging of SWIR and VNIR hyperspectral reflectance indices. Parameters were calculated as the mean value of all pixels from plant chlorophyll fluorescence imaging. DAE – day after emergency. Point represented mean ± SD (n = 9–15). Statistical differences are determined by Tukey *post-hoc* test and indicated as $p < 0.05$*, 0.01**, and 0.001***.

Figure 7: (a) Heatmap of coefficient of variability for individual plants phenotype traits affected by well-watered (WW) and water-stressed (WS) conditions. (b) Heatmap of Pearson correlation coefficient (r_P).

close dependence of ET, *A*, and plant water content (Water-1 index) on SWC (r_P > 0.80; p < 0.001). Other morphological traits (Comp, Round, RMS, Ecc, and Iso) were less correlated with water content (r_P = 0.20–0.40), except plant height (r_P = 0.63; p < 0.001). Functional traits of photosynthetic efficiency are characterized by high dependence on SWC (r_P = 0.50–0.73; p < 0.001), except Fv/Fm (r_P = 0.17).

4 Conclusions

Modern state-of-the-art high-throughput plant phenotyping (HTTP) is a technology that enables the simultaneous evaluation of a large number of traits. As demonstrated by the presented case study of tomato plants, the use of digital methods of plant imaging and calculation of structural and functional parameters has several advantages compared to classical methods of describing the phenotype. Digital imaging of optical signals from a plant is non-invasive and non-destructive and allows the evaluation of the plant's phenotype throughout its ontogeny. The digital imaging system made it possible to create databases of morpho-physiological features that are accessible for re-analysis and information sharing. Also, digital imaging allows several independent parameters to be calculated at once, increasing the overall predictive value of the phenotype realized in a particular environment. The study documented the

statistically significant complexity of the morphological and physiological responses of tomato plants affected by water stress. Plant geometric traits, especially Iso^{top}, Round-2^{top}, and $Comp^{side}$, showed a relatively low level of drought-induced phenotypic plasticity (PhP). On the other hand, functional and chemometric characteristics (especially parameters $\Delta F/F'm$, Rfd, Water-1, and ARI-1) showed the potential to exhibit rapid plasticity in WS conditions. Similarly, the experiments in tomato confirmed the reliability and repeatability of non-destructive HTTP quantification of individual morpho-physiological traits within individual repetitions (C.V. up to 0.20), especially under WS conditions. In conclusion, the quantification of the variability of individual traits in well-watered (WW) and water-stressed (WS) plants, as well as the phenotypic plasticity of traits and correlation analysis, point to the enormous potential of using digital phenotyping of plants affected by stress situations.

Funding information: This study was supported by the research projects of the Slovak Research and Development Agency APVV-SK-SRB-21-0043, APVV-20-0071, and APVV SK-CN-21-0045.

Author contributions: All authors have accepted responsibility for the entire content of this manuscript and consented to its submission to the journal, reviewed all the results. All authors have read and agreed to the published version of the manuscript. MK and MŽ; methodology, MK, MŽ, IV; software, MK; validation, MK, AF, and LJ; formal analysis, MK; investigation, MK and IV; resources, MK, IV, and DP; data curation, MK; writing – original draft preparation, MK; writing – review and editing, MŽ, MB, and XY; visualization, MK; supervision, MB and DP; project administration, MB, VB, and XY; funding acquisition, MB, VB, and XY.

Conflict of interest: Authors state no conflict of interest.

Data availability statement: Data sharing is not applicable to this article as no datasets were generated or analysed during the current study.

References

[1] Tardieu F, Simonneau T, Muller B. The physiological basis of drought tolerance in crop plants: A scenario-dependent probabilistic approach. Annu Rev Plant Biol. 2018;69(1):733–59. doi: 10.1146/annurev-arplant-042817-040218.

[2] Wheeler T, von Braun J. Climate change impacts on global food security. Science. 2013;341(6145):508–13. doi: 10.1126/science.1239402.

[3] Bashir SS, Hussain A, Hussain SJ, Wani OA, Zahid Nabi S, Dar NA, et al. Plant drought stress tolerance: Understanding its physiological, biochemical and molecular mechanisms. Biotechnol & Biotechnol Equip. 2021;35(1):1912–25. doi: 10.1080/13102818.2021.2020161.

[4] Lozano-Elena F, Fàbregas N, Coleto-Alcudia V, Caño-Delgado AI. Analysis of metabolic dynamics during drought stress in arabidopsis plants. Sci Data. 2022;9(1):90. doi: 10.1038/s41597-022-01161-4.

[5] Cardoso LL, Freire FBS, Daloso DM. Plant metabolic networks under stress: A multi-species/stress condition meta-analysis. J Soil Sci Plant Nutr. 2023;23(1):4–21. doi: 10.1007/s42729-022-01032-2.

[6] Favreau B, Gaal C, Pereira de Lima I, Droc G, Roques S, Sotillo A, et al. A multi-level approach reveals key physiological and molecular traits in the response of two rice genotypes subjected to water deficit at the reproductive stage. Plant-Environ Interact. 2023;4(5):229–57. doi: 10.1002/pei3.10121.

[7] Koch G, Rolland G, Dauzat M, Bédiée A, Baldazzi V, Bertin N, et al. Leaf production and expansion: A generalized response to drought stresses from cells to whole leaf biomass – A case study in the tomato compound leaf. Plants. 2019;8(10):409. doi: 10.3390/plants8100409.

[8] Li S, Liu J, Liu H, Qiu R, Gao Y, Duan A. Role of hydraulic signal and ABA in decrease of leaf stomatal and mesophyll conductance in soil drought-stressed tomato. Front Plant Sci. 2021;12:653186. doi: 10.3389/fpls.2021.653186.

[9] Chaves MM, Flexas J, Pinheiro C. Photosynthesis under drought and salt stress: Regulation mechanisms from whole plant to cell. Ann Bot. 2009;103(4):551–60. doi: 10.1093/aob/mcn125.

[10] Kalaji HM, Jajoo A, Oukarroum A, Brestic M, Zivcak M, Samborska IA, et al. Chlorophyll a fluorescence as a tool to monitor physiological status of plants under abiotic stress conditions. Acta Physiol Plant. 2016;38(4):102. doi: 10.1007/s11738-016-2113-y.

[11] Liang G, Liu J, Zhang J, Guo J. Effects of drought stress on photosynthetic and physiological parameters of tomato. J Am Soc Hortic Sci. 2020;145(1):12–7. doi: 10.21273/JASHS04725-19.

[12] Yang X, Li Y, Chen H, Huang J, Zhang Y, Qi M, et al. Photosynthetic response mechanism of soil salinity-induced cross-tolerance to subsequent drought stress in tomato plants. Plants. 2020;9(3):363. doi: 10.3390/plants9030363.

[13] Blum A. Osmotic adjustment is a prime drought stress adaptive engine in support of plant production. Plant Cell Environ. 2017;40(1):4–10. doi: 10.1111/pce.12800.

[14] Gupta A, Rico-Medina A, Caño-Delgado AI. The physiology of plant responses to drought. Science. 2020;368(6488):266–9. doi: 10.1126/science.aaz7614.

[15] Sousaraei N, Mashayekhi K, Mousavizadeh SJ, Akbarpour V, Medina J, Aliniaeifard S. Screening of tomato landraces for drought tolerance based on growth and chlorophyll fluorescence analyses. Hortic Env Biotechnol. 2021;62(4):521–35. doi: 10.1007/s13580-020-00328-5.

[16] Conti V, Parrotta L, Romi M, Del Duca S, Cai G. Tomato biodiversity and drought tolerance: A multilevel review. Int J Mol Sci. 2023;24(12):10044. doi: 10.3390/ijms241210044.

[17] Furbank RT, Tester M. Phenomics – Technologies to relieve the phenotyping bottleneck. Trends Plant Sci. 2011;16(12):635–44. doi: 10.1016/j.tplants.2011.09.005.

[18] Rebetzke GJ, Jimenez-Berni J, Fischer RA, Deery DM, Smith DJ. Review: High-throughput phenotyping to enhance the use of crop genetic resources. Plant Sci. 2019;282:40–8. doi: 10.1016/j.plantsci.2018.06.017.

[19] Watt M, Fiorani F, Usadel B, Rascher U, Muller O, Schurr U. Phenotyping: New windows into the plant for breeders. Annu Rev Plant Biol. 2020;71(1):689–712. doi: 10.1146/annurev-arplant-042916-041124.
[20] Yang W, Feng H, Zhang X, Zhang J, Doonan JH, Batchelor WD, et al. Crop phenomics and high-throughput phenotyping: Past decades, current challenges, and future perspectives. Mol Plant. 2020;13(2):187–214. doi: 10.1016/j.molp.2020.01.008.
[21] Fiorani F, Schurr U. Future scenarios for plant phenotyping. Annu Rev Plant Biol. 2013;64(1):267–91. doi: 10.1146/annurev-arplant-050312-120137.
[22] Poorter H, Hummel GM, Nagel KA, Fiorani F, von Gillhaussen P, Virnich O, et al. Pitfalls and potential of high-throughput plant phenotyping platforms. Front Plant Sci. 2023;14:1233794. doi: 10.3389/fpls.2023.1233794.
[23] Granier C, Aguirrezabal L, Chenu K, Cookson SJ, Dauzat M, Hamard P, et al. PHENOPSIS, an automated platform for reproducible phenotyping of plant responses to soil water deficit in Arabidopsis thaliana permitted the identification of an accession with low sensitivity to soil water deficit. N Phytol. 2006;169(3):623–35. doi: 10.1111/j.1469-8137.2005.01609.x.
[24] Jansen M, Gilmer F, Biskup B, Nagel KA, Rascher U, Fischbach A, et al. Simultaneous phenotyping of leaf growth and chlorophyll fluorescence via GROWSCREEN FLUORO allows detection of stress tolerance in Arabidopsis thaliana and other rosette plants. Funct Plant Biol. 2009;36(11):902–14. doi: 10.1071/FP09095.
[25] Nagel KA, Putz A, Gilmer F, Heinz K, Fischbach A, Pfeifer J, et al. GROWSCREEN-rhizo is a novel phenotyping robot enabling simultaneous measurements of root and shoot growth for plants grown in soil-filled rhizotrons. Funct Plant Biol. 2012;39(11):891–904. doi: 10.1071/FP12023.
[26] Chen D, Neumann K, Friedel S, Kilian B, Chen M, Altmann T, et al. Dissecting the phenotypic components of crop plant growth and drought responses based on high-throughput image analysis. Plant Cell. 2014;26(12):4636–55. doi: 10.1105/tpc.114.129601.
[27] Klukas C, Chen D, Pape J-M. Integrated analysis platform: An open-source information system for high-throughput plant phenotyping. Plant Physiol. 2014;165(2):506–18. doi: 10.1104/pp.113.233932.
[28] Al-Tamimi N, Brien C, Oakey H, Berger B, Saade S, Ho YS, et al. Salinity tolerance loci revealed in rice using high-throughput non-invasive phenotyping. Nat Commun. 2016;7(1):13342. doi: 10.1038/ncomms13342.
[29] Asaari MSM, Mertens S, Dhondt S, Inzé D, Wuyts N, Scheunders P. Analysis of hyperspectral images for detection of drought stress and recovery in maize plants in a high-throughput phenotyping platform. Computers Electron Agric. 2019;162:749–58. doi: 10.1016/j.compag.2019.05.018.
[30] Li D, Quan C, Song Z, Li X, Yu G, Li C, et al. High-throughput plant phenotyping platform (HT3P) as a novel tool for estimating agronomic traits from the lab to the field. Front Bioeng Biotechnol. 2021;13(8):623705. doi: 10.3389/fbioe.2020.623705.
[31] Ngo HTT, Cavagnaro TR, Jewell N, Brien CJ, Berger B, Watts-Williams SJ. High-throughput shoot phenotyping reveals temporal growth responses to nitrogen and inorganic and organic phosphorus sources in tomato. AoB Plants. 2023;15(2):plad011. doi: 10.1093/aobpla/plad011.
[32] Correia PMP, Cairo Westergaard J, Bernardes da Silva A, Roitsch T, Carmo-Silva E, Marques da Silva J. High-throughput phenotyping of physiological traits for wheat resilience to high temperature and drought stress. J Exp Bot. 2022;73(15):5235–51. doi: 10.1093/jxb/erac160.
[33] Corti M, Marino Gallina P, Cavalli D, Cabassi G. Hyperspectral imaging of spinach canopy under combined water and nitrogen stress to estimate biomass, water, and nitrogen content. Biosyst Eng. 2017;158:38–50. doi: 10.1016/j.biosystemseng.2017.03.006.
[34] Sytar O, Brestic M, Zivcak M, Olsovska K, Kovar M, Shao H, et al. Applying hyperspectral imaging to explore natural plant diversity towards improving salt stress tolerance. Sci Total Environ. 2017;578:90–9. doi: 10.1016/j.scitotenv.2016.08.014.
[35] Kovar M, Brestic M, Sytar O, Barek V, Hauptvogel P, Zivcak M. Evaluation of hyperspectral reflectance parameters to assess the leaf water content in soybean. Water. 2019;11(3):443. doi: 10.3390/w11030443.
[36] de Vylder J, Vandenbussche F, Hu Y, Philips W, Van Der Straeten D. Rosette tracker: An open source image analysis tool for automatic quantification of genotype effects. Plant Physiol. 2012;160(3):1149–59. doi: 10.1104/pp.112.202762.
[37] Tschiersch H, Junker A, Meyer RC, Altmann T. Establishment of integrated protocols for automated high throughput kinetic chlorophyll fluorescence analyses. Plant Methods. 2017;13(1):54. doi: 10.1186/s13007-017-0204-4.
[38] Jiang L, Sun L, Ye M, Wang J, Wang Y, Bogard M, et al. Functional mapping of N deficiency-induced response in wheat yield-component traits by implementing high-throughput phenotyping. Plant J. 2019;97(6):1105–19. doi: 10.1111/tpj.14186.
[39] Berger B, de Regt B, Tester M. High-throughput phenotyping of plant shoots. In: Normanly J, editor. High-throughput phenotyping in plants: Methods and protocols. Totowa, NJ: Methods in Molecular Biology; Humana Press; 2012. p. 9–20. doi: 10.1007/978-1-61779-995-2_2.
[40] Morota G, Jarquin D, Campbell MT, Iwata H. Statistical methods for the quantitative genetic analysis of high-throughput phenotyping data. Methods Mol Biol. 2022;2539:269–96. doi: 10.1007/978-1-0716-2537-8_21.
[41] Poudel S, Adhikari B, Dhillon J, Reddy KR, Stetina SR, Bheemanahalli R. Quantifying the physiological, yield, and quality plasticity of southern USA soybeans under heat stress. Plant Stress. 2023;9:100195. doi: 10.1016/j.stress.2023.100195.
[42] Fang Y, Xiong L. General mechanisms of drought response and their application in drought resistance improvement in plants. Cell Mol Life Sci. 2015;72(4):673–89. doi: 10.1007/s00018-014-1767-0.
[43] Blum A. Drought resistance – Is it a complex trait? Funct Plant Biol. 2011;38(10):753–7. doi: 10.1071/FP11101.
[44] Fricke W. Turgor pressure. In: Encyclopedia of life sciences. Chichester: John Wiley & Sons, Ltd; 2017. p. 1–6. doi: 10.1002/9780470015902.a0001687.pub2.
[45] Gratani L. Plant phenotypic plasticity in response to environmental factors. Adv Bot. 2014;2014:e208747. doi: 10.1155/2014/208747.
[46] Janni M, Coppede N, Bettelli M, Briglia N, Petrozza A, Summerer S, et al. In vivo phenotyping for the early detection of drought stress in tomato. Plant Phenomics. 2019;2019:6168209. doi: 10.34133/2019/6168209.
[47] Junker A, Muraya MM, Weigelt-Fischer K, Arana-Ceballos F, Klukas C, Melchinger AE, et al. Optimizing experimental procedures for quantitative evaluation of crop plant performance in high throughput phenotyping systems. Front Plant Sci. 2015;5:770. doi: 10.3389/fpls.2014.00770.
[48] Bi H, Kovalchuk N, Langridge P, Tricker PJ, Lopato S, Borisjuk N. The impact of drought on wheat leaf cuticle properties. BMC Plant Biol. 2017;17(1):85. doi: 10.1186/s12870-017-1033-3.

[49] Zhou R, Kong L, Wu Z, Rosenqvist E, Wang Y, Zhao L, et al. Physiological response of tomatoes at drought, heat and their combination followed by recovery. Physiol Plant. 2019;165(2):144–54. doi: 10.1111/ppl.12764.
[50] Amitrano C, Junker A, D'Agostino N, De Pascale S, De Micco V. Integration of high-throughput phenotyping with anatomical traits of leaves to help understanding lettuce acclimation to a changing environment. Planta. 2022;256:68. doi: 10.1007/s00425-022-03984-2.
[51] Baker NR. Chlorophyll fluorescence: A probe of photosynthesis in vivo. Annu Rev Plant Biol. 2008;59(1):89–113. doi: 10.1146/annurev.arplant.59.032607.092759.
[52] Banks JM. Chlorophyll fluorescence as a tool to identify drought stress in acer genotypes. Environ Exp Botany. 2018;155:118–27. doi: 10.1016/j.envexpbot.2018.06.022.
[53] Živčák M, Brestič M, Olšovská K, Slamka P. Performance index as a sensitive indicator of water stress in Triticum aestivum L. Plant Soil Environ. 2008;54(4):133–9. doi: 10.17221/392-PSE.
[54] Moles TM, Mariotti L, De Pedro LF, Guglielminetti L, Picciarelli P, Scartazza A. Drought induced changes of leaf-to-root relationships in two tomato genotypes. Plant Physiol Biochem. 2018;128:24–31. doi: 10.1016/j.plaphy.2018.05.008.
[55] Carvalho FEL, Ware MA, Ruban AV. Quantifying the dynamics of light tolerance in arabidopsis plants during ontogenesis. Plant Cell Environ. 2015;38(12):2603–17. doi: 10.1111/pce.12574.
[56] Ghorbanzadeh P, Aliniaeifard S, Esmaeili M, Mashal M, Azadegan B, Seif M. Dependency of growth, water use efficiency, chlorophyll fluorescence, and stomatal characteristics of lettuce plants to light intensity. J Plant Growth Regul. 2021;40(5):2191–207. doi: 10.1007/s00344-020-10269-z.
[57] Lichtenthaler HK, Buschmann C, Knapp M. How to correctly determine the different chlorophyll fluorescence parameters and the chlorophyll fluorescence decrease ratio RFd of leaves with the PAM fluorometer. Photosynthetica. 2005;43(3):379–93. doi: 10.1007/s11099-005-0062-6.
[58] Conti V, Romi M, Parri S, Aloisi I, Marino G, Cai G, et al. Morpho-physiological classification of Italian tomato cultivars (Solanum Lycopersicum L.) according to drought tolerance during vegetative and reproductive growth. Plants. 2021;10(9):1826. doi: 10.3390/plants10091826.